# Resonant exciton excitation photoluminescence and dynamics in a GaAs/AlAs multiple quantum well with internal electric field

Kojima, Osamu
Kita, Takashi
Steer, Matthew J.
Hogg, Richard A.

(Citation)
AIP Advances,10(9):095016-095016

(Issue Date)
2020-09-01

(Resource Type)
journal article

(Version)
Version of Record

# Resonant exciton excitation photoluminescence and dynamics in a GaAs/AlAs multiple quantum well with internal electric field

Cite as: AIP Advances **10**, 095016 (2020); https://doi.org/10.1063/5.0020177
Submitted: 28 June 2020 . Accepted: 21 August 2020 . Published Online: 14 September 2020

Osamu Kojima, Takashi Kita, Matthew J. Steer, and Richard A. Hogg

# Resonant exciton excitation photoluminescence and dynamics in a GaAs/AlAs multiple quantum well with internal electric field

Cite as: AIP Advances 10, 095016 (2020); doi: 10.1063/5.0020177
Submitted: 28 June 2020 • Accepted: 21 August 2020 •
Published Online: 14 September 2020



Osamu Kojima,[1,a] Takashi Kita,[1] Matthew J. Steer,[2] and Richard A. Hogg[2]

## AFFILIATIONS

[1] Department of Electrical and Electronic Engineering, Graduate School of Engineering, Kobe University, 1-1 Rokkodai, Nada, Kobe 657-8501, Japan
[2] Electronics and Nanoscale Engineering, James Watt School of Engineering, University of Glasgow, Glasgow G12 8LT, United Kingdom

[a] Author to whom correspondence should be addressed: kojima@phoenix.kobe-u.ac.jp

## ABSTRACT

The stability of excitons with large oscillator strengths at room temperature has been of great significance in device applications. In this paper, we report the effects of the ultrafast dissociation of excitons confined in a quantum well on optical characteristics. The photoluminescence spectra show components of higher energy than the excitation energy and a nonlinear increment of the intensity. Furthermore, the spectrally resolved pump–probe signals at the exciton energies elucidate the change in the exciton position. These results indicate the importance of the exciton stability in optical devices, in particular emission type, including terahertz wave, based on excitons.



## I. INTRODUCTION

Resonant exciton excitation induces strong light absorption and emission because of its large oscillator strength, which is an important property for the development of optical device applications as well as fundamental physics. For instance, ultrafast response,[1–5] Rabi oscillation,[6–11] emission of the terahertz (THz) wave,[12–14] and polariton laser emission[15] have been the pressing topics for the development of devices based on excitons confined in the semiconductor nanostructures. In particular, for these optically controlled devices, their dynamics and interaction with other excitons and carriers under exciton excitation conditions should be understood. Recently, wide frequency tunability of the THz wave generated by difference frequency mixing (DFM) processes using exciton transitions in a multiple quantum well (MQW)[16,17] was demonstrated. In the measurements, the heavy-hole (HH) exciton was excited by one laser, and the second laser energy was tuned. Although the THz signal demonstrated the HH exciton resonant effect, the signal was not significantly enhanced at the light-hole (LH) exciton energy. When the intensity of the THz signal simply depended on the two exciton oscillator strengths, the signal was expected to be enhanced at the LH exciton energy. This is because the light absorption is larger than the other excitation energies. Therefore, it is difficult to simply discuss the magnitude of second-order nonlinear polarization by the absorption, i.e., exciton oscillator strengths. In particular, considering the Pauli exclusion principle, the broadened resonant effect seems to correspond to the interaction between the excitons in different positions within the inhomogeneous width.

Meanwhile, there are various reports on exciton dynamics under resonant excitation at room temperature. Here, focusing on the excitons in GaAs quantum wells, for instance, the nonlinear excitonic response at room temperature,[18–20] rapid bleaching recovery related to the optical Stark effect,[21] the response caused by the excitation of the HH exciton,[22] and the enhancement of the pump–probe signal at the LH exciton energy and increase of the ultrafast decay component ratio at the HH exciton energy[23] were reported. These previous reports have focused on the strong oscillator strength of

excitons. To further enhance the intensity of the THz wave, effects of the interaction between the spatially separated excitons, including within the inhomogeneous line width, should be clarified. Therefore, in this paper, we discuss the interaction between the spatially separated excitons from the photoluminescence (PL) spectra measured under resonant exciton excitation conditions and the spectrally resolved (SR) exciton dynamics. The PL intensities show a nonlinear increase at room temperature, which results from the ultrafast exciton dissociation. The variation of the SR pump–probe signals supports that the exciton dissociation modifies the optical properties.

## II. EXPERIMENT

We used an undoped GaAs/AlAs MQW embedded in a p-i-n structure on a (001) $n^+$-doped GaAs substrate grown by a molecular-beam epitaxy. The thickness of the surface $p$-doped GaAs layer with a doping concentration of $1 \times 10^{18}$ cm$^{-3}$ is 50 nm, and that of the bottom $n$-doped GaAs layer with a doping concentration of $3 \times 10^{18}$ cm$^{-3}$ is 1500 nm. The MQW consists of 30 periods of GaAs and AlAs layers whose thickness is 7.25 nm. The schematic of the sample structure is given in Fig. 1. To measure the PL spectrum, a continuous-wave mode Ti:sapphire laser was used as the excitation light source in normal incidence. The excitation energy was tuned from 1.504 eV to 1.566 eV. In the case of this energy region, 25% of the laser light reaches at the bottom well.[24] The luminescence was measured by a 35-cm single monochromator with a 0.2 nm resolution connected to a charge-coupled device. The transient response was measured using a reflection-type pump–probe technique. The light source was a mode-locked Ti:sapphire pulse laser with a pulse width of approximately 100 fs and a repetition rate of 80 MHz. The pump energy was tuned in the exciton energy region. The pump power was kept at 1.2 $\mu$J/cm$^2$. To measure the SR pump–probe signals, a 10-cm single monochromator with a resolution of 1.3 nm was used to resolve the probe-light spectrum. All measurements were performed at a room temperature of 296 K.

## III. RESULTS AND DISCUSSION

First, the effects of exciton dissociation on the PL spectrum are discussed. The potential difference between the first and the 30th well is ~700 meV, which was estimated from the internal field of 16 kV/cm by the doping concentrations of p- and n-layers and the i-layer thickness of 435 nm, as indicated in Fig. S1. The barrier width of 7.25 nm is sufficient to confine the electron and holes, and the calculated miniband widths of electron and holes are zero. Therefore, the tunneling probabilities are very low.

Figure 2 indicates the PL spectrum under the non-resonant excitation conditions. The fitting results used to obtain the origins of each component are indicated by the dotted curves. To fit, the combination of the Gaussian and Lorentzian functions was used. Here, the Lorentzian function was used for the HH exciton peak, while the Gaussian function was used for the other peaks. The origins of the PL peaks were speculated from the lower energy side, surface p-layer, HH, 2s, LH, and HH2. The peak energy of the p-layer was estimated from the spectrum measured by very weak excitation under non-resonant excitation conditions. The peaks labeled as HH and LH originate from the HH and LH excitons, respectively. The peak energy of the 2s exciton[25–29] was estimated from the low-temperature PL spectra, and that of HH2, which indicates the transition between the second HH and first electron states, was evaluated from the photoreflectance spectrum. The Lorentzian function was only used for the HH exciton peak because of the ultrafast dephasing caused by the ionization.[19] We tried several combinations

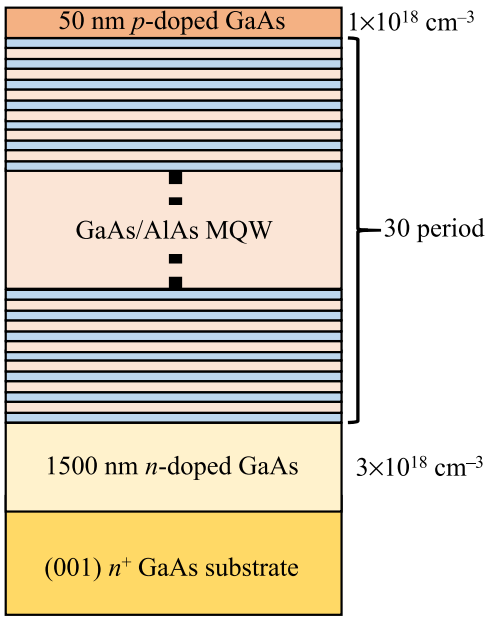


**FIG. 1**. Schematic of the sample structure.

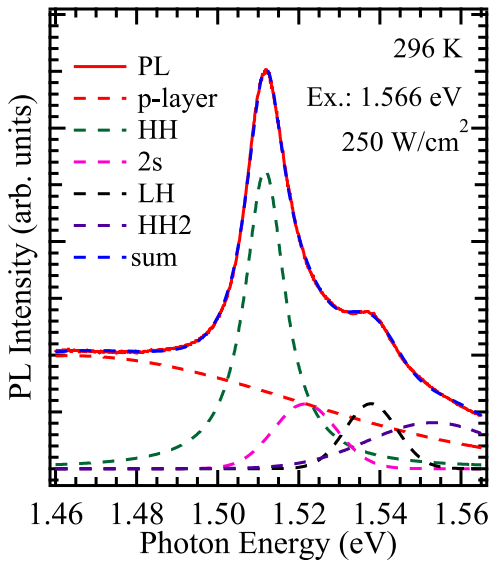


**FIG. 2**. PL spectrum measured at 296 K. The fitting results are indicated by the dotted curves.

of functions; however, we got the best fitting in the case where only the HH exciton is fitted by the Lorentz function.

The PL spectra measured at various excitation energies are shown in Fig. 3. The excitation energies are indicated by the triangles in each PL spectrum. Although the carriers initially have no kinetic energy in the case of normal incidence resonant excitation, the PL spectra show higher components than the excitation energy; the exciton population distributed to the higher energy sides. The higher energy PL components were observed at low excitation power and room temperature, which suggests that the two-step excitation mediated by the virtual states, electron–hole pairs and/or phonon[30–32] and the carrier distribution excited by the nonlinear process in the surface and buffer layers[33] hardly contribute to the PL components.

To eliminate the possibility of an effect related to state filling on the population distribution from the discussion, the dependences of the PL spectrum on the excitation power were measured. The dependences at the excitation energies of 1.504 eV corresponding to the non-resonant excitation, 1.511 eV, and 1.540 eV are shown in Figs. 4(a)–4(c), respectively. The energies of 1.511 eV and 1.540 eV correspond to the HH and LH exciton energies, respectively. The spectra do not include the offset (no shift of spectra); thus, the PL intensities show a nonlinear increase even in the case where the excitation energy is lower than the exciton energies. The PL intensities at the HH and LH exciton energies do not show the saturation because of the large exciton decay rate at room temperature; therefore, the state filling can be ignored as the origin of exciton of higher states compared with the excitation energy.

To clarify the excitation-power dependence of the PL intensities, all spectra were analyzed by fitting, based on the model mentioned above. The intensities of the PL components, the p-layer, HH, 2s, LH, and HH2 excitons, are plotted in Figs. 5(a) and 5(b) for the conditions of HH and LH exciton excitation, respectively. The dotted lines indicate the gradients of linear and square dependences for the excitation density. The intensity of the HH exciton is lower than the others, which results from the HH exciton peak being fitted using the Lorentzian function. Except for the intensity of the p-layer indicated by the open circles showing linear dependence, the intensities increase for the square of excitation density. The change in the gradient obtained by fitting is shown in Table I of the supplementary material.

Furthermore, the PL intensities at the HH and LH excitons, obtained by the various excitation energies, are plotted as a function of excitation density in Figs. 6(a) and 6(b), respectively. Although the intensities seem to approach the linear dependence in the higher excitation density region, the intensity shows the square dependence. The change in the gradient obtained by fitting is also shown in Table II of the supplementary material. The square dependence on the excitation density originates from the ultrafast dissociation of excitons, reported in quantum wells and quantum dots.[34–39] Because the dissociation is shorter than the exciton formation time, the disappearance of the electron or hole in an electron–hole pair and exciton leads to a nonlinear intensity increase.[40]

The higher-energy PL components result from the exciton dissociation. Considering the thermal energy of room temperature, the origin of PL is not only the simple thermal excitation. The higher

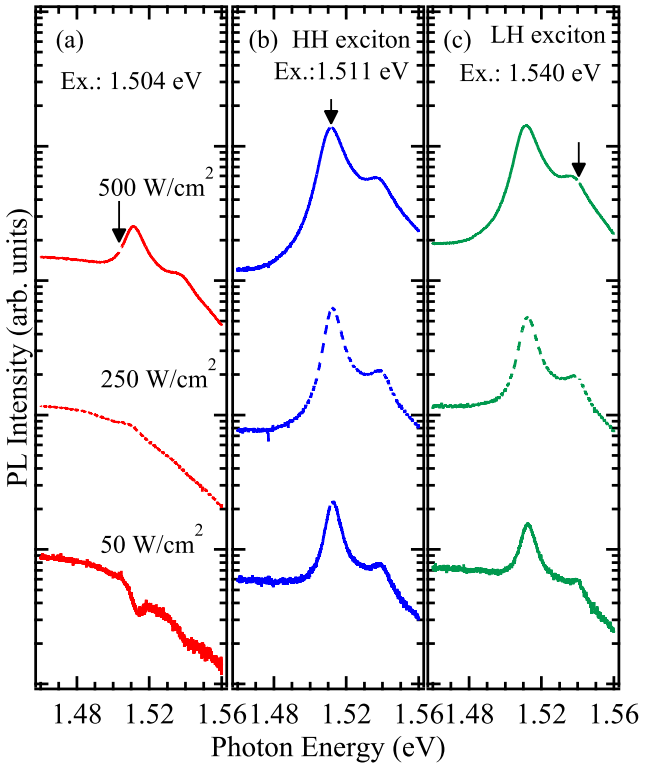


**FIG. 4**. Excitation density dependence of the PL spectrum. The excitation energies of (a) 1.504 eV, (b) 1.511 eV, and (c) 1540 eV are indicated by the arrows.

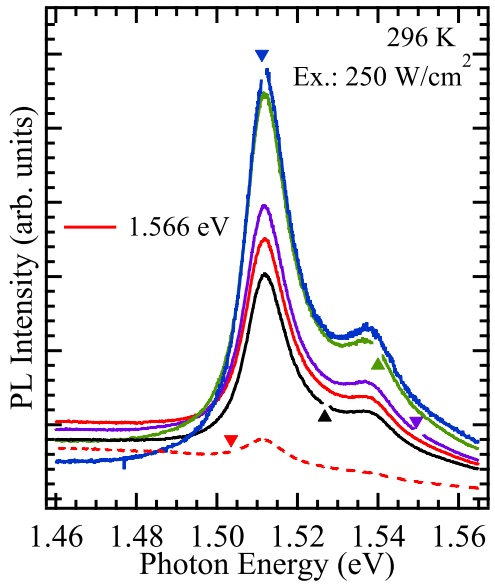


**FIG. 3**. Excitation energy dependence of the PL spectrum. The triangles indicate the excitation energies of 1.5035 eV, 1.5112 eV, 1.5268 eV, 1.5400 eV, and 1.5495 eV from left to right.

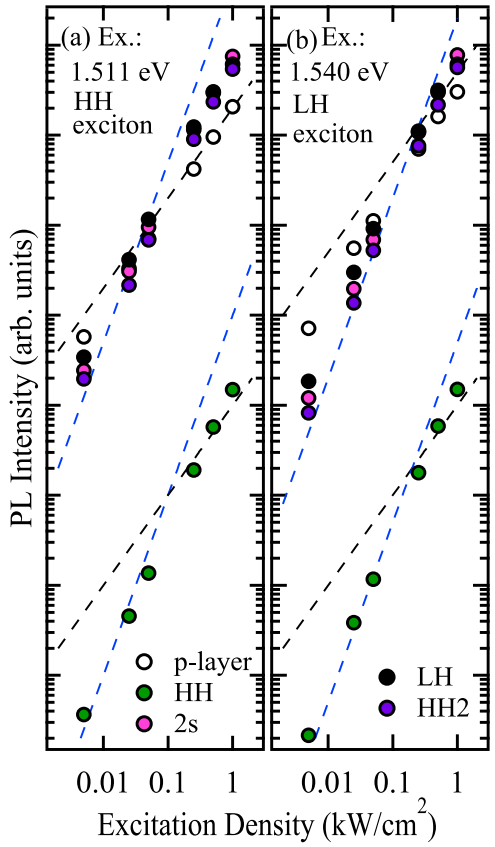


**FIG. 5**. Excitation density dependence of the PL intensities excited at (a) HH and (b) LH exciton energies. The dotted lines indicate the gradients of linear and square.

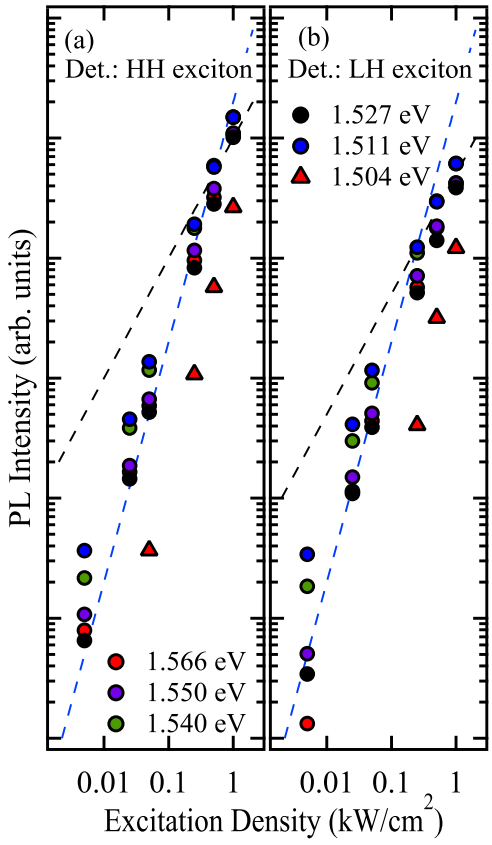


**FIG. 6**. Excitation density dependence of the PL intensities detected at (a) HH and (b) LH exciton energies. The dotted lines indicate the gradients of linear and square.

energy PL was observed in the lower excitation density, which indicates that the elastic and inelastic scatterings are not the origin. Here, the penetration depth of the light of 1.50 eV is ~800 nm,[41] for the bottom n-layer to be excited. Therefore, in the case of the excitation energy of 1.504 eV, the electron generated in the p-layer and the hole generated in the n-layer move to QWs by tunneling and recombine. Moreover, in the cases of the exciton resonant excitation, tunneling of the electron and hole of the dissociated exciton to the next wells causes PL. As mentioned above, the tunneling probability is very low; however, it is not zero. In particular, under the electric field, the transmittance is increased. Thus, the tunneling of the electron and holes of the dissociated exciton causes the higher-energy PL.

Next, the effects of the exciton dissociation on the dynamics under resonant excitation are discussed. We measured the SR pump–probe signals under the HH-exciton excitation condition, as shown in Fig. 7(a). Figure 7(b) indicates the numerical summation of SR signals, which corresponds to the usual pump–probe signal. The spectral position of the signal detection in the exciton peak is shown in Fig. S2. Here, the time-domain signals include the offset to align along with the detection energy. The signals detected at the higher energy side first show an intensity reduction and recovery after the minimum. On the other hand, the signals detected at the lower energy side show an increase in intensity. The decrease in the signal intensity in the higher energy side seems to correspond to the increase in the intensity in the lower energy side.

To discuss the exciton dynamics in the spectral region, the integrated signal intensities are plotted as a function of photon energy in Fig. 8. Here, each point indicates the summation of the signal intensity without the offset in the indicated time duration of 200 fs. For the reference, the PL spectrum is indicated by the solid curve.

On the higher energy side, the signal intensity decreases from −200 to 0 fs as indicated by the open circles and increases after 0 fs. On the other hand, on the lower energy side, the signal intensities increase from 0 fs; the intensity is maintained. These results demonstrate that the excitons in the higher energy components shift to the lower energy positions. This is attributed to the excitons moving to different (thicker) thickness positions within the inhomogeneous (well width fluctuations) well. This movement causes the ionization and dephasing of the exciton.

The same measurement was performed at the LH exciton energy to clarify the effect of the intersubband transition, as shown in Fig. 9. The signal-to-noise ratio is not as high; however, the dynamics are different from the results obtained at the HH exciton

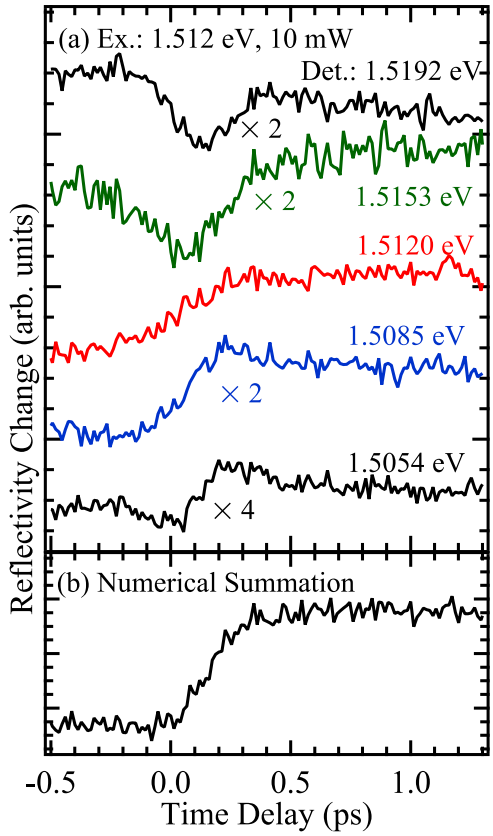


**FIG. 7**. (a) SR pump–probe signals. All signals include the offset to align by the order of detection energy. (b) Numerical summation of the SR signals.

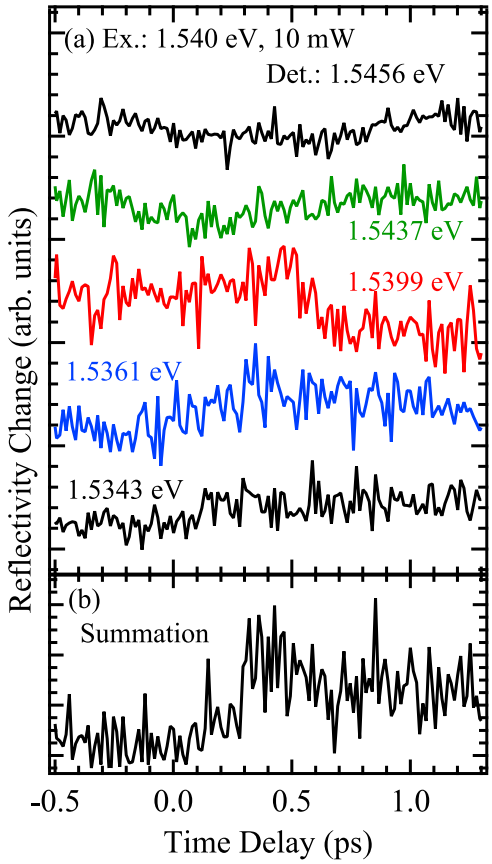


**FIG. 9**. (a) SR pump–probe signals measured at the LH exciton energy. All signals include the offset to align by the order of detection energy. (b) Numerical summation of the SR signals.

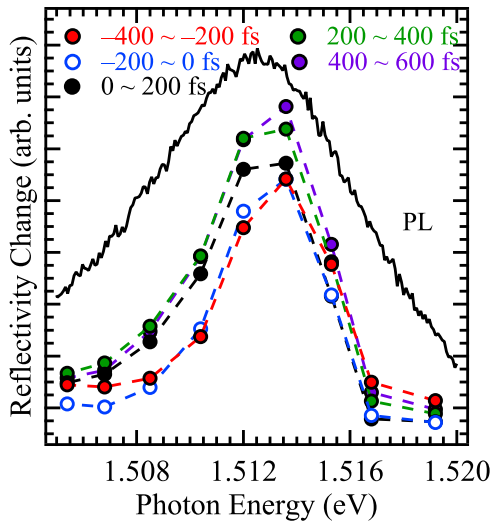


**FIG. 8**. Integrated signal intensities of the time duration of 200 fs and PL spectrum.

energy. This difference is attributed to the LH state having another relaxation path to the HH state. Namely, in the case of the LH exciton, the intersubband transition causes the ionization/dephasing more effectively.

Furthermore, the integrated intensities are plotted as a function of photon energy at various time durations for discussion of the dynamics in Fig. 10. In comparison with the change in the lower energy side, the change in the higher energy side is small, which is contrary to the result at the HH exciton energy. Furthermore, the recovery of the intensity of the higher energy side components, which appeared in the case of the HH exciton energy, was not observed. This result indicates that the interaction of the LH excitons within the inhomogeneous width is not observed due to the intersubband transition to the HH state.

We now discuss the evaluated peak widths. The widths of the HH and LH exciton PL peaks in Fig. 2 are 12 meV and 21.3 meV, respectively, which were evaluated from the fitting mentioned above. Meanwhile, the peak width of the reflectivity change in Fig. 8 was 5.0 meV, and that in Fig. 10 was 9.4 meV. Considering the relationship of the homogeneous and inhomogeneous widths, $\Gamma^2 = \Gamma^2_{inh} + \Gamma^2_{hom}$,[42] the values obtained from the reflectivity change correspond

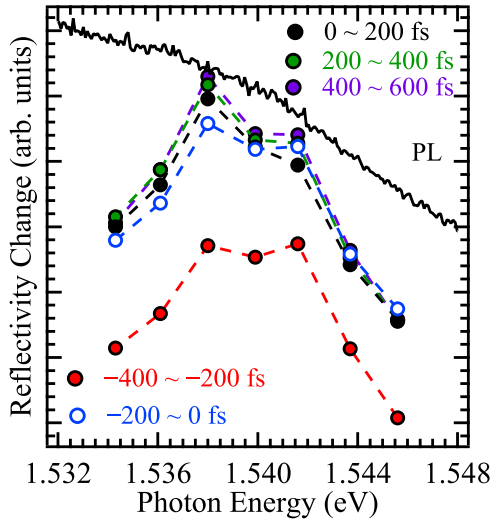


**FIG. 10**. Integrated signal intensities of the time duration of 200 fs and PL spectrum.

to the inhomogeneous width $\Gamma_{inh}$, which has little dependence on temperature. The estimated homogeneous widths $\Gamma_{hom}$ of HH and LH excitons from the relationship are 11 meV and 20 meV, respectively, where the widths obtained from the PL analysis were used as Γ. Therefore, the larger $\Gamma_{hom}$ values suggest more rapid exciton dephasing.

Finally, the relationship between the exciton generation and optical nonlinearity is discussed. In the excitation-power dependence of the PL intensities, the exciton PL shows a linear increase above the excitation density of 1 kW/cm$^2$. On the other hand, the nonlinear THz signals demonstrated the threshold behavior around 2 or 5 kW/cm$^2$ in Ref. 16. To generate the THz wave, the stable nonlinear polarization due to the excitons is required. When the excitation power is lower, the probability of the exciton overlap to create the second nonlinear polarization is low. With the increase in the excitation power, the exciton is stably created and the probability of overlap increases. Therefore, the stable exciton creation is important in generating the strong THz wave due to the DFM process.

## IV. CONCLUSION

We investigated the effects of the exciton dissociation on the exciton dynamics at room temperature by studying the resonantly and non-resonantly excited PL spectra, including the excitation density dependence, and the SR pump–probe signals measured at the HH and LH exciton energies. The PL spectra show components larger than the excitation energy, and the PL intensities demonstrated a nonlinear increase with increasing excitation density. The SR pump–probe signals at the HH exciton energy demonstrated the carrier movement toward the lower energies, which was not observed in excitation of the LH exciton. These results indicate that ultrafast exciton dissociation causes the ultrafast dephasing in the weak excitation power region. Therefore, the realization of optical devices based on excitonic effects requires the stable generation of excitons.

## SUPPLEMENTARY MATERIAL

See the supplementary material for the band diagram for electron, HH and LH subbands under the internal electric field, laser spectra, and values of gradient obtained by fitting.

## ACKNOWLEDGMENTS

We would like to acknowledge the financial support provided by JSPS KAKENHI Grant Nos. 26289088 and 16KK0129, the JSPS International Research Fellow (Graduate School of Engineering, Kobe University), the Masuya-Kinen Basic Research Foundation, the Hyogo Foundation for Science and Technology, and the Support Center for Advanced Telecommunications Technology Research Foundation.

## DATA AVAILABILITY

The data that support the findings of this study are available from the corresponding author upon reasonable request.

## REFERENCES

[1] J. Feldmann and E. Göbel, Appl. Phys. Lett. **57**, 1520 (1990).
[2] H. Nakamura, K. Kanamoto, Y. Nakamura, S. Ohkouchi, H. Ishikawa, and K. Asakawa, J. Appl. Phys. **96**, 1425 (2004).
[3] O. Kojima, T. Isu, J. Ishi-Hayase, A. Kanno, R. Katouf, M. Sasaki, and M. Tsuchiya, J. Phys. Soc. Jpn. **77**, 044701 (2008).
[4] C. Y. Jin, O. Kojima, T. Kita, O. Wada, M. Hopkinson, and K. Akahane, Appl. Phys. Lett. **95**, 021109 (2009).
[5] O. Kojima, K. Hayashii, T. Kita, and K. Akahane, J. Phys. D: Appl. Phys. **47**, 105101 (2014).
[6] T. H. Stievater, X. Li, D. G. Steel, D. Gammon, D. S. Katzer, D. Park, C. Piermarocchi, and L. J. Sham, Phys. Rev. Lett. **87**, 133603 (2001).
[7] A. Zrenner, E. Beham, S. Stufler, F. Findeis, M. Bichler, and G. Abstreiter, Nature **418**, 612 (2002).
[8] H. Htoon, T. Takagahara, D. Kulik, O. Baklenov, A. L. Holmes, Jr., and C. K. Shih, Phys. Rev. Lett. **88**, 087401 (2002).
[9] M. Kujiraoka, J. Ishi-Hayase, K. Akahane, N. Yamamoto, K. Ema, and M. Sasaki, Appl. Phys. Express **3**, 092801 (2010).
[10] T. Yamashita, O. Kojima, T. Kita, and K. Akahane, J. Appl. Phys. **110**, 043514 (2011).
[11] D. Wigger, C. Schneider, S. Gerhardt, M. Kamp, S. Höfling, T. Kuhn, and J. Kasprzak, Optica **5**, 1442 (2018).
[12] M. Bieler, K. Pierz, U. Siegner, and P. Dawson, Phys. Rev. B **76**, 161304 (2007).
[13] S. Priyadarshi, M. Leidinger, K. Pierz, A. M. Racu, U. Siegner, M. Bieler, and P. Dawson, Appl. Phys. Lett. **95**, 151110 (2009).
[14] K. Morita, S. Katoh, T. Takimoto, F. Tanaka, Y. Nakagawa, S. Saito, T. Kitada, and T. Isu, Appl. Phys. Express **4**, 102102 (2011).
[15] S. I. Tsintzos, P. G. Savvidis, G. Deligeorgis, Z. Hatzopoulos, and N. T. Pelekanos, Appl. Phys. Lett. **94**, 071109 (2009).
[16] O. Kojima, Y. Tarui, H. Shimazu, T. Kita, A. Majeed, P. Ivanov, E. Clarke, and R. Hogg, Phys. Rev. Appl. **10**, 044035 (2018).
[17] A. Majeed, P. Ivanov, B. Stevens, E. Clarke, I. Butler, D. Childs, O. Kojima, and R. Hogg, Light: Sci. Appl. **8**, 29 (2019).
[18] W. H. Knox, R. L. Fork, M. C. Downer, D. A. B. Miller, D. S. Chemla, C. V. Shank, A. C. Gossard, and W. Wiegmann, Phys. Rev. Lett. **54**, 1306 (1985).
[19] D. S. Chemla and D. A. B. Miller, J. Opt. Soc. Am. B **2**, 1155 (1985).
[20] W. H. Knox, D. A. B. Miller, T. C. Damen, D. S. Chemla, C. V. Shank, and A. C. Gossard, Appl. Phys. Lett. **48**, 864 (1986).

[21] S. G. Lee, P. A. Harten, J. P. Sokoloff, R. Jin, B. Fluegel, K. E. Meissner, C. L. Chuang, R. Binder, S. W. Koch, G. Khitrova, H. M. Gibbs, N. Peyghambarian, J. N. Polky, and G. A. Pubanz, Phys. Rev. B **43**, 1719 (1991).
[22] A. M. T. Kim, S. Hunsche, T. Dekorsy, H. Kurz, and K. Köhler, Appl. Phys. Lett. **68**, 2956 (1996).
[23] T.-A. Liu, J.-M. Shieh, K.-F. Huang, and C.-L. Pan, Jpn. J. Appl. Phys., Part 1 **42**, 5869 (2003).
[24] O. Kojima, R. Izumi, and T. Kita, J. Phys. D: Appl. Phys. **51**, 305102 (2018).
[25] K. J. Moore, P. Dawson, and C. T. Foxon, Phys. Rev. B **34**, 6022 (1986).
[26] T. Hayakawa, K. Takahashi, M. Kondo, T. Suyama, S. Yamamoto, and T. Hijikata, Phys. Rev. B **38**, 1526 (1988).
[27] L. W. Molenkamp, G. E. W. Bauer, R. Eppenga, and C. T. Foxon, Phys. Rev. B **38**, 6147 (1988).
[28] W. M. Theis, G. D. Sanders, C. E. Leak, D. C. Reynolds, Y.-C. Chang, K. Alavi, C. Colvard, and I. Shidlovsky, Phys. Rev. B **39**, 1442 (1989).
[29] D. W. Kim, Y. A. Leem, S. D. Yoo, D. H. Woo, D. H. Lee, and J. C. Woo, Phys. Rev. B **47**, 2042 (1993).
[30] S. C. Hohng and D. S. Kim, Appl. Phys. Lett. **75**, 3620 (1999).
[31] P. P. Paskov, P. O. Holtz, and P. Petroff, Appl. Phys. Lett. **77**, 812 (2000).
[32] R. Bhattacharya, B. Pal, and B. Bansal, Appl. Phys. Lett. **105**, 191102 (2014).
[33] S. Machida, T. Tadakuma, A. Satake, and K. Fujiwara, J. Appl. Phys. **98**, 083527 (2005).
[34] J. E. Fouquet and A. E. Siegman, Appl. Phys. Lett. **46**, 280 (1985).
[35] K. Fujiwara, N. Tsukada, and T. Nakayama, Appl. Phys. Lett. **53**, 675 (1988).
[36] O. Brandt, K. Kanamoto, M. Gotoda, T. Isu, and N. Tsukada, Phys. Rev. B **51**, 7029 (1995).
[37] E. C. Le Ru, J. Fack, and R. Murray, Phys. Rev. B **67**, 245318 (2003).
[38] Y. D. Jang, J. Park, D. Lee, D. J. Mowbray, M. S. Skolnick, H. Y. Liu, M. Hopkinson, and R. A. Hogg, Appl. Phys. Lett. **95**, 171902 (2009).
[39] T. Kita, R. Hasagawa, and T. Inoue, J. Appl. Phys. **110**, 103511 (2011).
[40] R. Strobel, R. Eccleston, J. Kuhl, and K. Köhler, Phys. Rev. B **43**, 12564 (1991).
[41] M. D. Sturge, Phys. Rev. **129**, 2835 (1963).
[42] D. Gammon, S. Rudin, T. L. Reinecke, D. S. Katzer, and C. S. Kyono, Phys. Rev. B **51**, 16785 (1995).